

9 Element Strategy Initiative to Form Core Research Center for Electron Materials

– Multi probe study using X-rays, muons and neutrons –

*Youichi Murakami, Hiroshi Kumigashira,
Kenji Kojima, Hitoshi Abe, Jun-ichi Yamaura*

9-1 Introduction

The national project “Elements strategy initiative to form core research center for electron materials” was started in 2012. We are aiming to develop entirely new materials that use ubiquitous elements. We are developing materials based on successful experience far away from development policy, and are pioneering electronic materials to create new guidelines for material design using harmless elements to open up new fields of material science. We are researching the crystal, local, electronic, and magnetic structures of new functional materials using synchrotron radiation, muon and neutron sources.

9-2 Hydrogen ordering and new polymorph of layered perovskite oxyhydrides: $\text{Sr}_2\text{VO}_{4-x}\text{H}_x$

Compositionally tunable layered perovskite vanadium oxyhydrides $\text{Sr}_2\text{VO}_{4-x}\text{H}_x$ ($0 \leq x \leq 1.01$) without considerable anion vacancy were synthesized by high-pressure solid state reaction. The crystal structures and their properties were characterized by powder neutron diffraction, synchrotron X-ray diffraction, thermal desorption spectroscopy, and first-principles density functional theory (DFT) calculations. The hydrogen anions selectively replaced equatorial oxygen sites in the VO_6 layers via statistical substitution of hydrogen in the low x region ($x < 0.2$) (Fig. 1). A new orthorhombic phase (Immm) with an almost entirely hydrogen-ordered structure formed from the K_2NiF_4 -type tetragonal phase with $x > 0.7$. This indicates a drastic change of physical properties from the two-dimensional d^1 magnet to the one-dimensional d^2 magnet [1].

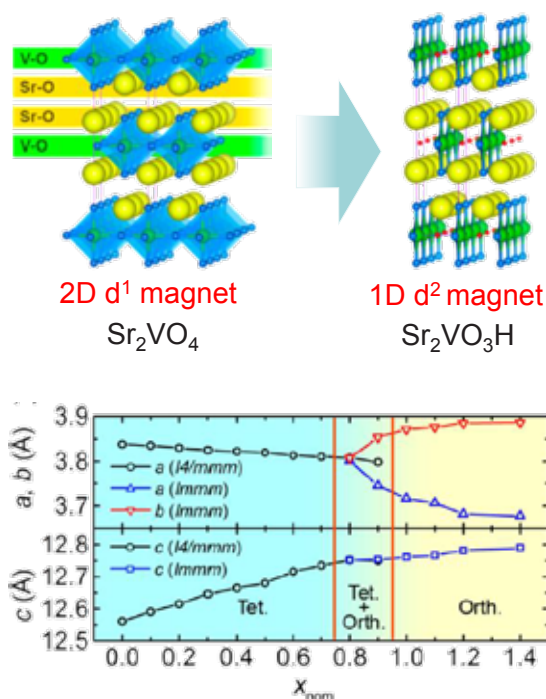


Fig. 1: Crystal structure transformation from the layered perovskite Sr_2VO_4 , two-dimensional (2D) d^1 magnet to the one-dimensional (1D) d^2 magnet. The material obtained by doping hydrogen anions heavily crystallizes in a new polymorph of the orthorhombic phase.

9-3 Determination of band diagram for a p-n junction between Mott insulator LaMnO_3 and band insulator Nb:SrTiO_3

The band diagram of epitaxial p-n junctions between the Mott insulator with p-type carriers LaMnO_3 and the n-type semiconductor Nb-doped SrTiO_3 (Nb:STO) was obtained using X-ray photoemission spectroscopy. With the donor concentration in Nb:STO ranging from 0.1 at. % to 1.0 at. %, the value of the built-in potential for the Nb:STO side (V_{bn}) is reduced from 0.55 eV to 0.25 eV. The modulation of V_{bn} is well described in the

framework of the conventional p-n junction model. These results suggest that the characteristics of perovskite oxide p-n junctions can be predicted and designed using the transport properties of the constituent oxides, irrespective of their strongly correlated electronic nature (Fig. 2) [2].

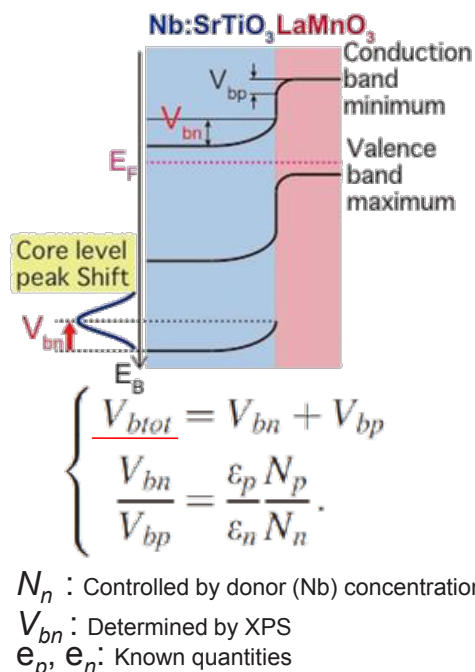


Fig. 2: Band diagrams of LMO/Nb:STO heterojunctions deduced from the present XPS measurements. The built-in potentials and carrier concentrations for conventional p-n junctions are given by the equations.

9-4 Direct growth of metallic TiH₂ thin films by pulsed laser deposition

The layer-by-layer growth and electronic properties of (111)-oriented TiH₂ films (δ -phase) pulsed-laser-deposited on α -Al₂O₃(0001) using a TiH₂ ceramic target were investigated. The content of the δ -phase increased as the decomposition to the Ti metal was suppressed at low temperatures. Moreover, long-lasting oscillations of reflection high-energy electron diffraction intensity were observed during the initial growth of the δ -phase film. The film showed metallic conductivity down to low temperatures. The results of Ti 2p–3d resonant photoemission spectroscopy and Hall measurement were consistent with those of the conducting electrons residing in the Ti 3d states (Fig. 3) [3].

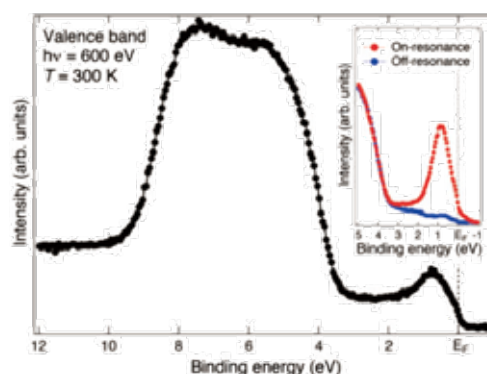


Fig. 3: Valence band spectrum of the TiH_{1.9} film. The inset shows Ti 2p–3d on- and off-resonant photoemission spectra near E_F taken at photon energies of 459 and 452 eV, respectively.

9-5 Bipolarity of germanium in layered BaM₂Ge₄Ch₆ (M = Rh, Ir and Ch = S, Se) with pyrite-type building blocks

Layered compounds BaM₂Ge₄Ch₆ (M = Rh, Ir; Ch = S, Se) were synthesized under high pressure, and the structure as well as chemical features were studied (Fig. 4). These compounds crystallize in a new structure type with space group Pbc_a. Their remarkable structure features the M-Ge-Ch pyrite-type building unit which stacks with BaCh layers alternately along the c-axis. Theoretical calculation and experimental results indicate that there is a strongly polarized covalent bond between Ge and Ch atoms. Moreover, Ge atoms in this structure exhibit unusual bipolar behavior due to the different electronegativity of Rh, Ge and Ch and the special coordination environment of Ge atoms along with

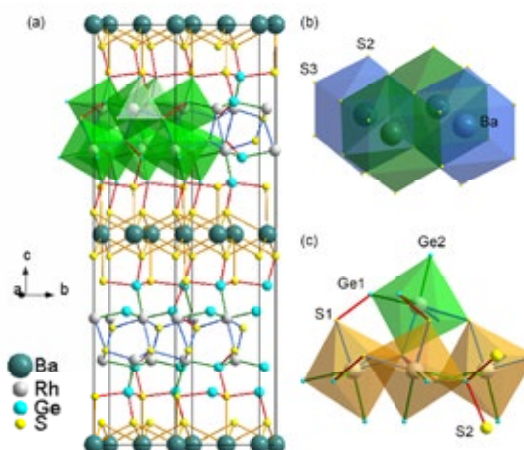


Fig. 4: (a) Structure of BaRh₂Ge₄S₆. The octahedron of Rh-Ge/S is emphasized. The atoms are marked as follows: Ba, dark cyan; Rh, white; Ge, light blue; S, yellow. (b) The view of a section of the Ba-S layer. Ba is located in the dodecahedron of S. (c) The view of part of the Rh-Ge/S layer. The Ge1-S1 bond is labeled in red.

Rh and Ch simultaneously. Theoretical calculation indicates that all of them are semiconductors [4].

9-6 New photoemission beamline construction for the element strategy project

We constructed the new “Musashi” beamline BL-2 to promote research for the element strategy project. High flux and high energy resolution beams over a wide energy range of 30–2,000 eV are realized by the dual lines with vacuum ultraviolet (30–300 eV) and soft X-ray (250–2,000 eV) (Fig. 5). X-ray absorption spectroscopy of all elements can be performed. The band structure can be determined by angle-resolved photoemission spectroscopy, and the chemical bonding state can be evaluated by inner shell photoelectron spectroscopy.

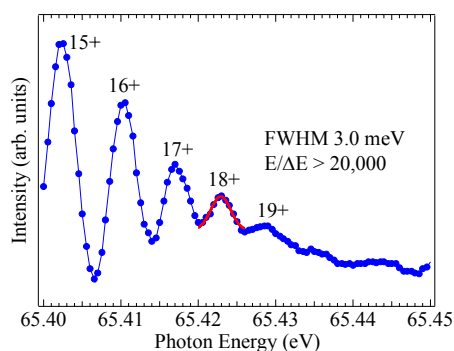


Fig. 5: New “tandem” beamline BL-02, “Musashi” (Multiple Undulator beamline for Spectroscopic Analysis of Surface and Hetero Interface). Photoionization spectrum of the gas-phase He indicates the resolution performance of FWHM 3.0 meV and $E/\Delta E > 20000$.

9-7 Installation of a new spectrometer at S-line: muon spin relaxation measurements for the element strategy project

In the “S1 experimental area” at J-PARC MLF, we installed the new spectrometer and detector for the element strategy project (Fig. 6). The big bore spectrometer can be utilized for various



Fig. 6: New spectrometer for the muon spin relaxation measurement installed at the S1 experimental area.

experiments, while the new detector “KALLIOPE” is an innovative system for detecting positrons with a pixel-avalanche photodiode, which reduces the sensitivity to the magnetic field and also the size of the system. The commissioning of the beamline and the spectrometer will start in the autumn of 2015.

References

- [1] Hydrogen Ordering and New Polymorph of Layered Perovskite Oxyhydrides: $\text{Sr}_2\text{VO}_{4-x}\text{H}_x$, J. Bang, S. Matsuishi, H. Hiraka, F. Fujisaki, T. Otomo, S. Maki, J. Yamaura, R. Kumai, Y. Murakami, H. Hosono, *J. Am. Chem. Soc.* **136**, 7221 (2014).
- [2] Determination of band diagram for a p-n junction between Mott insulator LaMnO_3 and band insulator Nb:SrTiO_3 , M. Kitamura, M. Kobayashi, E. Sakai, R. Takahashi, M. Lippmaa, K. Horiba, H. Fujioka, H. Kumigashira, *Appl. Phys. Lett.* **106**, 061605 (2015).
- [3] Direct Growth of Metallic TiH_2 Thin Films by Pulsed-Laser Deposition, K. Yoshimatsu, T. Suzuki, N. Tsuchimine, K. Horiba, H. Kumigashira, T. Oshima, A. Ohtomo, *Appl. Phys. Express* **8**, 035801 (2015).
- [4] Layered Compounds $\text{BaM}_2\text{Ge}_4\text{Ch}_6$ ($M = \text{Rh, Ir}$ and $\text{Ch} = \text{S, Se}$) with Pyrite-Type Building Blocks and Ge–Ch Heteromolecule-Like Anions, H. Lei, J. Yamaura, J. Guo, Y. Qi, Y. Toda, H. Hosono, *Inorg. Chem.* **53**, 5684 (2014).